UV-Initiated Free Radical and Cationic Photopolymerizations of Acrylate/Epoxide and Acrylate/Vinyl Ether Hybrid Systems with and without Photosensitizer

Jung-Dae Cho, Jin-Who Hong

Department of Polymer Science and Engineering, Chosun University, Gwangju 501–759, South Korea

Received 28 April 2003; accepted 29 February 2004
DOI 10.1002/app.20597
Published online in Wiley InterScience (www.interscience.wiley.com).

ABSTRACT: Various properties of UV-initiated acrylate/epoxide and acrylate/vinyl ether hybrid photopolymerizations with and without photosensitizer in the presence of free radical and cationic-type photoinitiators have been determined by dynamic mechanical thermal analysis (DMTA), calorimetric analysis (photodifferential scanning calorimetry, photo-DSC; and differential scanning calorimetry), and scanning electron microscopy. DMTA experiments revealed that the UV curing of hybrid systems may produce interpenetrating polymer networks. Photo-DSC analyses indicated that the acrylates polymerized faster than the epoxide and vinyl ether in the hybrid systems; the addition of a photosensitizer, isopropylthioxanthone (ITX), increased the polymerization rate of the epoxide and vinyl ether in the hybrid systems. SEM analysis confirmed that the free radical system seemed to be significantly affected by oxygen inhibition, while the cationic and hybrid systems were not nearly inhibited by oxygen; the presence of photosensitization produced by the addition of ITX enhanced the surface curing of the hybrid systems. © 2004 Wiley Periodicals, Inc. J Appl Polym Sci 93: 1473–1483, 2004

Key words: photopolymerization; hybrid system; photosensitizer; calorimetry; electron microscopy

INTRODUCTION

Free radical and cationic UV-curable photopolymerizations have received considerable attention for the rapid, solvent-free curing of coating films. Such polymerizations have been in constant development over the last 30 years, due to their advantages in important industrial applications, including adhesives, coatings, inks, varnishes, and electronics.[1–4]

Until recently, most studies on UV-initiated photopolymerizations have focused on free radical systems (RSs) based primarily upon acrylates. These acrylates polymerize rapidly and are easily modified to provide multifunctionality, allowing materials with greatly different properties to be obtained. However, acrylates are relatively volatile, inhibited by oxygen, have an unpleasant odor, exhibit high viscosities, and present potential health hazards, including carcinogenicity.[5–7] Therefore, acrylate monomers are being substituted in many formulations by vinyl ethers (VEs). The main advantages of using VE with acrylate are lower odor and skin irritancy, without sacrificing cure speed relative to the common acrylate monomers. It has been reported that coatings produced from acrylate/VE (A/VE) hybrid systems (HSs) involving the two mechanisms of UV-induced free radical and cationic polymerization exhibit physical properties—such as solvent resistance or impact strength—that are superior to those of acrylates alone.[8–10]

Cationically UV-initiated photopolymerizations exhibit several advantages over the free radical photopolymerizations discussed above. The cationic photopolymerizations based mainly on epoxides and VEs are not inhibited by oxygen, have low shrinkage during curing, and exhibit relatively low viscosities and negligible toxicity. Furthermore, the low shrinkage of cycloaliphatic epoxides produces better adhesion on substrates with low absorption, such as metal and certain plastics. However, despite all their advantages, their market share is small, which is probably attributable to their reactivity being lower than that of the acrylates and to their sensitivity toward environmental factors such as temperature and moisture.[11] One possible method for overcoming these disadvantages of cationic-photoinitiated systems is to introduce an acrylate/epoxide (A/E) HS into the UV-curable formulations. This hybrid formulation system is more reactive in polymerization and less sensitive to moisture than cationic formulations alone.[12,13]

Many hybrid coating systems have already been reported, but to our knowledge there are no detailed reports on such systems that contain photosensitizer.

Correspondence to: J.-W. Hong (jhhong@mail.chosun.ac.kr).

Free-radical photoinitiator

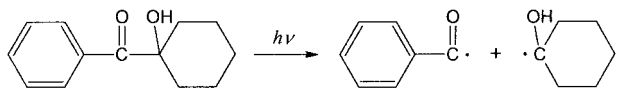

Cationic photoinitiator

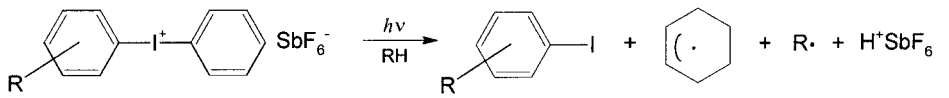

Figure 1 Photochemical decomposition of the free radical and cationic photoinitiators.

The study described here used photodifferential scanning calorimetry (photo-DSC), scanning electron microscopy (SEM), and dynamic mechanical thermal analysis (DMTA) to investigate the effect of the photosensitizer isopropylthioxanthone (ITX) on the physical properties, kinetics behaviors, and surface morphology of A/E and A/VE HSs.

EXPERIMENTAL

Materials

Aliphatic urethane acrylate (UA, Ebecryl 9970, UCB Chemicals) and 3,4-epoxycyclohexyl-methyl-3,4-epoxycyclohexane carboxylate (CADE, Uvacure 1500, UCB Chemicals) were used as the resin. Trimethylolpropane triacrylate (TMPTA, Sartomer) and 1,4-cyclohexane dimethanol divinyl ether (CHVE, RAPI-CURE, International Specialty Products) were used as a reactive diluent. 1-Hydroxy-cyclohexyl-phenyl ketone (Irgacure 184, Ciba-Geigy) and diaryliodonium hexafluoroantimonate (CD-1012, Sartomer) were used as a free radical and cationic photoinitiator, respectively. The ITX photosensitizer used was Firstcure ITX (First Chemical Corp.). LA-D490 (Tego Chemical Service) was used as a dispersant. All the materials were used as received. It should be noted here that the photolysis of the free radical photoinitiator (Irgacure 184) produces a benzoyl radical and an α-hydroxyalkyl radical, both of which are capable of reacting with the acrylate double bond, and the photolysis of the cationic photoinitiator (CD-1012) in the presence of a hydrogen donor molecule (RH) produces both protonic species (Brönsted acid) and free radicals, of which protonic acid initiates the cationic polymerization as shown in Figure 1.[1,6]

Coating formulation, curing procedure, and film property tests

The liquid coating formulations listed in Table I were applied to a glass substrate using a wire-wound rod, and the wet films were exposed to UV radiation at a conveyor speed of 5 m/min using an 80 W/cm medium-pressure mercury lamp and conventional UV equipment. The number of passes to achieve thorough cure was from 1 to 3. To evaluate the surface and curing properties of the cured films, pencil hardness and methyl ethyl ketone (MEK) double-rub tests were conducted according to the standard ASTM methods D3363–74 and D4752, respectively. The test method of pencil hardness is practiced by pushing a number of pencils that decrease in hardness along the coating. The pencils must have a flattened end and they must be held at an angle of 45° against the film. The hardness of the first pencil not to dig into or gouge the film is used to denote the hardness of the film. Pencils vary in the scale of hardness from 6B to 6H. The test method of MEK double-rubs is the resistance to a solvent-soaked cloth rubbed across the coated surface until the coating has been rubbed away. The degree of cure is ascertained by counting the number of double rubs—a back-and-forth motion over the test area of $\sim$ 50 mm. In addition, pendulum hardness (ASTM D4366) was measured from the damping of the oscillations of a pendulum from an angle of 6° to 3° (König ref. 707KP, Sheen). The König pendulum is a triangular open framework with an adjustable counterbalance weight. The pendulum assembly weighs 200 $\pm$ 0.2 g and pivots on two ball bearings 5 mm in diameter that rest on the test surface. The period of oscillation is 1.4 $\pm$ 0.02 s. Pendulum hardness values are expressed in seconds and are related directly to the softness of the sample. The shorter the damping time, the lower the

TABLE I
Formulations of the Cationic, Free Radical, and Hybrid Systems with Varying Types and Amounts of Photoinitiators and Photosensitizer

Coating component	CS (%)	RS (%)	HS1 (%)	HS2 (%)	HS1-P (%)	HS2-P (%)
CADE (epoxy carboxylate)[a]	60	—	60	—	60	—
CHVE (alcohol vinyl ether)[b]	40	—	—	40	—	40
UA (urethane acrylate)[c]	—	60	—	60	—	60
TMPTA (alcohol acrylate)[d]	—	40	40	—	40	—
CD-1012 (photoinitiator)[e]	3	—	1.8	1.2	1.8	1.2
Irgacure 184 (photoinitiator)[f]	—	3	1.2	1.8	1.2	1.8
ITX (photosensitizer)[g]	—	—	—	—	0.5	0.5
LA-D490 (dispersant)[h]	0.5	0.5	0.5	0.5	0.5	0.5

[a] UCB Chemicals (Uvacure 1500).
[b] International Specialty Products (RAPI-CURE).
[c] UCB Chemicals (Ebecryl 9970).
[d] Sartomer.
[e] Sartomer.
[f] Ciba-Geigy.
[g] First Chemical Corporation (Firstcure ITX).
[h] Tego Chemical Service.

hardness. The film properties were measured 24 h after UV exposure.

Izod impact tests

The notched Izod impact strength of the coated polycarbonates was measured by an ITR-2000 impact tester at room temperature (23°C). The size of the notched rectangular specimens was $64 \times 13 \times 3$ mm^3, and the impact pressure was 600 kPa. The photopolymerizable system was coated onto both polycarbonate surfaces at a thickness of ~ 45 μm and cured by UV radiation at a conveyor speed of 5 m/min using a 80 W/cm medium-pressure mercury lamp. The number of passes to achieve thorough cure was from 1 to 3. Each reported measurement represents the average value of five measurements.

Swelling tests

Swelling was assessed by measuring differences in weight between the dried film and the swollen film. For accurate measurement of the weight of the dried film, the original films were immersed in MEK for 48 h to remove impurities from the film surface and unreacted materials and then dried to a constant weight in a vacuum oven for 48 h. The weight of the film swollen with solvent was measured immediately after blotting the film between sheets of filter paper. Tests were made with three samples of each film. The following equation was used to calculate the swelling ratio:

$$\text{Swelling (\%)} = \frac{W_s - W_d}{W_d} \times 100 \qquad (1)$$

where W_s and W_d are the weight of the swollen and dried films, respectively.

Dynamic mechanical thermal analysis

Dynamic mechanical analysis was performed using a dynamic mechanical thermal analyzer (Mark II, Polymer Laboratories) at a frequency of 1 Hz in the tensile mode. The samples used for DMTA measurements were cured by UV radiation at a conveyor speed of 5 m/min using a 80-W/cm medium-pressure mercury lamp until thorough curing was achieved. Typically the cured film had dimensions of $24 \times 7 \times 0.3$ mm^3. Storage moduli (E') and loss tangents (tan δ) were obtained as a function of temperature at a constant heating rate of 1°C/min.

UV-visible spectroscopy

Absorption spectra of the photoinitiators (Irgacure 184 and CD-1012) and photosensitizer (ITX) were obtained using a Cary 3 Bio UV-visible spectrophotometer. Dilutions of 0.02 g/L in methylene chloride were prepared, and quart cells with a path length of 1.0 cm were used in the analysis.

Photo-differential scanning calorimetry

The photo-DSC experiments were conducted using a differential scanning calorimeter equipped with a photocalorimetric accessory (TA 5000/DPC System, TA Instruments). The initiation light source was a 200-W high-pressure mercury lamp: the UV light intensity at the sample was 35 mW/cm^2 over a wavelength range of 200–440 nm. The samples were placed

TABLE II
Properties of the Films Formulations in Table I as Measured at Room Temperature 24 h after the UV Curing[a]

Physical property	CS	RS	HS1	HS2	HS1-P	HS2-P
Pencil hardness	F	2B	F	HB	F	F
Pendulum hardness (s)	210	179	218	179	229	209
MEK double rubs	71	15	58	34	65	51
Izod impact test; break energy (J)	48	56	45	59	42	50
Number of passes to achieve thorough cure[b]	3	1	1	1	1	1

[a] The general cure conditions described in Sect-2 were used. Curing room conditions were 22–25°C with 25–30% relative humidity. Film thickness: ~ 45 μm.

[b] The films (~ 45 μm) were coated onto glass substrate and exposed to a 80 W/cm mercury vapor lamp at a conveyor speed of 5 m/min. The number of passes required to achieve thorough curing was recorded.

in uncovered aluminum pans (weight ~ 4.0 mg and thickness ~ 500 μm). TA Instruments software was employed to obtain the results from the photo-DSC experiments.

Differential scanning calorimetry

The DSC experiments were carried out on the UV-cured samples using a TA Instruments DSC 2010 immediately after the photo-DSC experiments. The samples that were UV cured during photo-DSC were covered with an aluminum pan. The sample weight was ~ 4.0 mg. The cell was first cooled down to –20°C and then heated to 250°C at a constant rate of 10°C/min. The data were analyzed using TA Instruments software.

Scanning electron microscopy

The surface morphology of the UV-cured films was observed using SEM (Hitachi S-4700) with an accelerating voltage of 25 kV.

RESULTS AND DISCUSSION

Characterization of the cationic, free-radical, and hybrid systems

The formulations of the cationic system CS, RS, and HSs with varying types and amounts of photoinitiators and photosensitizer are listed in Table I. A wire-wound drawdown rod was used to apply the formulations to glass substrate, and the coatings were cured under the general cure conditions outlined in Section 2 (22–25°C and 25–30% relative humidity).

Table II presents the typical physical properties of the various formulations listed in Table I. These data were obtained at room temperature 24 h after the UV curing. Comparing the results in Table II for the CS and RS formulations, it can be seen that the CS gave better pencil hardness and MEK solvent resistance than did the RS, which indicates that the crosslink density at the surface of the CS is superior to that of the RS due to the absence of oxygen inhibition that is common to RSs. The CS also gave higher pendulum hardness (which is inversely related to the softness) and lower break energy (which is related to the impact toughness) than did the RS, which implies that the crosslink density at the interior of the CS is superior to that of the RS due to the dark curing, which is a distinct characteristic of cationic photopolymerizations.[14–16] However, the RS exhibited much faster curing than did the CS.

The results in Table II indicate the limitations of the CS and RS. The main problem with the CS is slower curing, which is probably attributable to the low efficiency of the initiation process; the main problem of the RS is oxygen inhibition, which causes inferior surface curing of these photopolymerizations. These limitations can be overcome by introducing free-radical/cationic HSs into the UV-curable formulations.[6,8–10] For this reason, we prepared acrylate/epoxide (HS1) and acrylate/vinyl ether (HS2) HSs in the presence of free radical and cationic-type photoinitiators and investigated their physical properties and curing rates.

Table II clearly indicates that the HS1 system formulated using CADE with TMPTA instead of CHVE gave a higher extent of cure and faster curing than did the CS system. This behavior may be explained by considering that, during the early polymerization of the acrylate monomer, the CADE epoxide—which is still liquid at that stage—acts as a plasticizer, which will increase the conversion and cure rate of the TMPTA acrylate to form a polymer film that is stiffer than that of the CS.[6]

Figure 2 shows plots of pendulum hardness and break energy versus film thickness for the HS1. Not surprisingly, this figure demonstrates that, as the film thickness is increased, the pendulum hardness of the film decreases whereas the break energy increases, which means that the thicker the film, the lower the crosslink density of the UV-cured film.

On the other hand, the HS2 system formulated using UA with CHVE instead of TMPTA exhibited better surface curing and toughness than did the RS system. In such an A/VE HS containing free radical and cationic photoinitiators, enhanced surface curing is at-

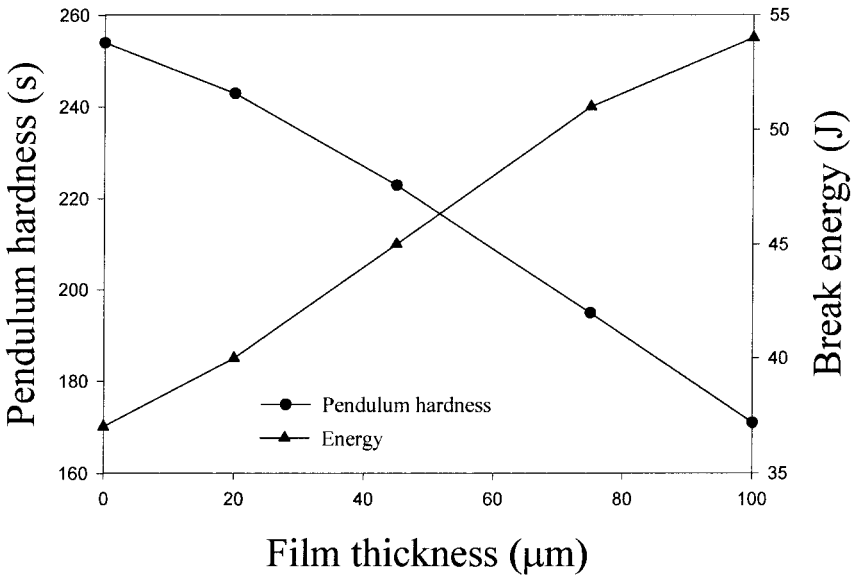

Figure 2 Plot of pendulum hardness (König) and break energy versus film thickness for the acrylate/epoxide system (HS1).

tributable to minimization of the inhibitory effect of oxygen by the VE monomer polymerizing cationically or radically; enhanced toughness is accounted for by the VE monomer increasing the chain mobility of the crosslinked copolymer formed. It should be noted that the electron-donor VE monomers are known to undergo a radical-type copolymerization with electron-acceptor monomers, such as acrylates or maleimides, when they are exposed to UV radiation. In this A/VE HS, the VE monomer is acting both as a reactive diluent to lower the formulation viscosity and as a plasticizer of the acrylate polymer network formed to increase its molecular mobility. The film obtained upon UV curing of the A/VE (HS2) HS consists of two interpenetrating polymer networks (IPNs). One is a VE-crosslinked homopolymer formed by a cationic mechanism; the other is a VE–acrylate copolymer with isolated VE units, because VE double bonds do not homopolymerize by a free-radical mechanism; e.g., see Decker and Decker:[8]

–A–A–VE–A–VE–A–A–A–A–VE–A–A–VE–A–VE–A–A–A–

Figure 3 shows the storage modulus and loss tangent of A/E (HS1) and A/VE (HS2) HSs as a function of temperature. The data from DMTA analysis are collected in Table III. The crosslink density of the hybrids was calculated based on the storage modulus in the rubbery plateau region according to:[17,18]

$$XLD = \frac{E'}{3RT} \tag{2}$$

where XLD is the crosslink density, E' is the elastic storage modulus in the rubbery plateau region, R is the ideal gas constant, and T is the temperature in kelvin.

The glass transition temperature of a polymeric material is the temperature at which the micro-Brownian movements of the molecular chain segments become significant. Therefore, any responses of the material to a particular chemical and physical environment mainly occur at or above the glass transition temperature, and hence, the higher the glass transition temperature, the better the chemical and physical resistance.[18,19] Careful examination of Figure 3 and Table III reveals that the glass transition temperature, the elastic storage modulus, and the crosslink density of the HS1 formulation were higher than those of HS2, clearly indicating that HS1 produced a harder film than did HS2. This trend may be ascribed to the fact that cycloaliphatic epoxides generally yield coatings that are intrinsically hard and brittle.[11,14] These results from the DMTA analysis are consistent with the pendulum hardness and the break energy of the HSs, as described in Table II.

At this point it should be mentioned that the HS1 and HS2 hybrids each exhibited two glass transition temperatures, which reflects that the UV curing of these two HSs produced IPNs via both free radical and cationic mechanisms.

Photosensitized polymerization of the hybrid systems

We also prepared A/E and A/VE HSs containing a photosensitizer (HS1-P and HS2-P, respectively) to investigate the influence of a photosensitizer on the physical properties and the photopolymerization kinetics.

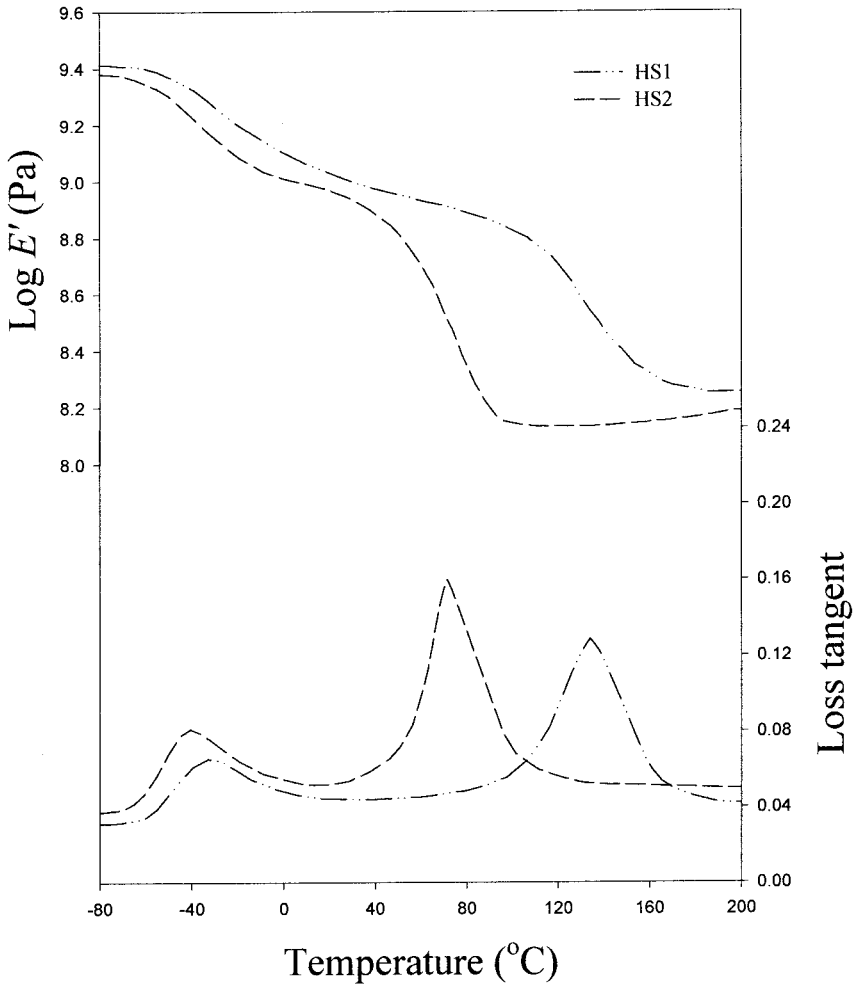

Figure 3 Storage modulus (E') and loss tangent (tan δ) of the UV-cured hybrid systems (HS1, HS2) as a function of temperature, as monitored using DMTA (measured at 1 Hz).

Figure 4 shows the comparison of pendulum hardness and break energy for the HSs with and without ITX photosensitizer. From Figure 4 and Table II, it can be also seen that the polymerizations of the HSs photosensitized with ITX photosensitizer exhibited higher pendulum hardness and MEK solvent resistance and lower break energy than did the HSs without ITX photosensitizer, indicating that the systems containing photosensitizer formed more highly crosslinked network films. The better performance of formulations HS1-P and HS2-P is due to photosensitization: the efficiency of the photoinitiator was improved to give more active species.[5] This photosensitization occurs via an excited state complex (exciplex) as a result of a direct interaction between an excited state of a photosensitizer and the photoinitiator and proceeds by an energy- or electron-transfer mechanism to form a radical cation that is capable of initiating free radical and cationic photopolymerizations.[14–16,20,21] In general, thioxanthones have been used to photosensitize both free radical and cationic photopolymerizations.[22–24]

TABLE III
Dynamic Mechanical Thermal Analysis Data for the Hybrid Systems (HS1 and HS2)

Formulation	Temperature at tan δ (°C)		$E'^{a} \times 10^{8}$ (Pa)	XLD[b] $\times 10^{4}$ (mol/cm^3)
	Low	High		
HS1	−33	134	2.6	2.25
HS2	−40.5	71.5	1.7	1.47

[a] The storage modulus in the rubbery region after the glass transitions.
[b] The crosslink density (XLD) was calculated at 463K.

Absorption spectra for the photoinitiators (Irgacure 184, CD-1012) and photosensitizer (ITX) are depicted in Figure 5. The absorption of the photoinitiators peaks in the 240–300 nm region and that of the ITX photosensitizer peaks in the 360–400 nm region with a secondary peak in the 240–300 nm region. Due to this stronger absorption by ITX, including it as a photosensitizer may enlarge the initiating wavelength for

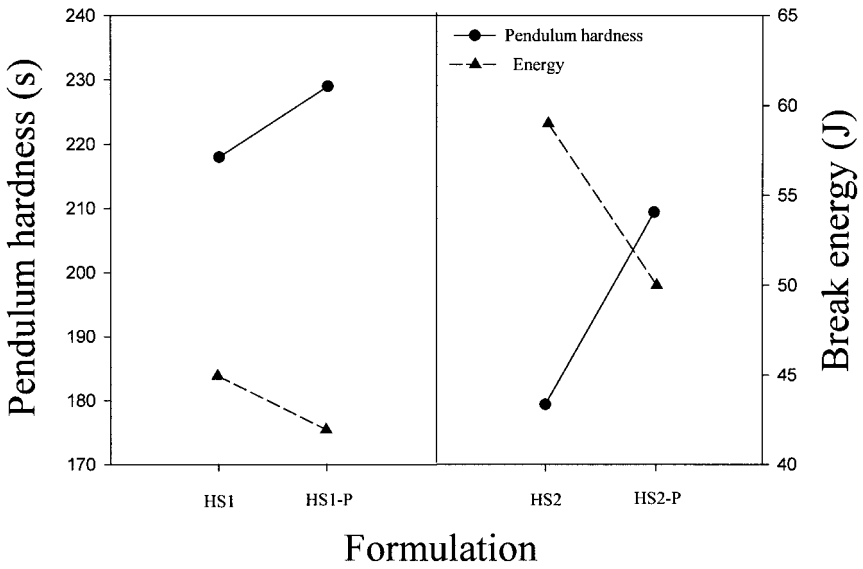

Figure 4 Comparison of pendulum hardness (König) and break energy for the hybrid systems with and without photosensitizer (HS1, HS1-P: acrylate/epoxide system; HS2, HS2-P: acrylate/vinyl ether system).

the photopolymerization, thereby improving the efficiency of the initiation process.

Swelling measurements also show that a tighter network was achieved with the formulations containing the ITX photosensitizer (Fig. 6). The lower swelling ratio of the photosensitized HSs (HS1-P, HS2-P) confirms that highly crosslinked IPNs were formed upon the UV curing of these systems. These results correlate well with the pendulum hardness and impact test results.

Kinetic analysis of the photopolymerizations

The photopolymerization kinetics was analyzed using photo-DSC to clarify the photocuring process of the systems listed in Table I. Photo-DSC experiments are capable of providing kinetics data in which the measured heat flow can be converted directly to the ultimate percentage conversion and polymerization rate for a given amount of formulation, with the data obtained reflecting the overall curing reaction of the sample.[25,26]

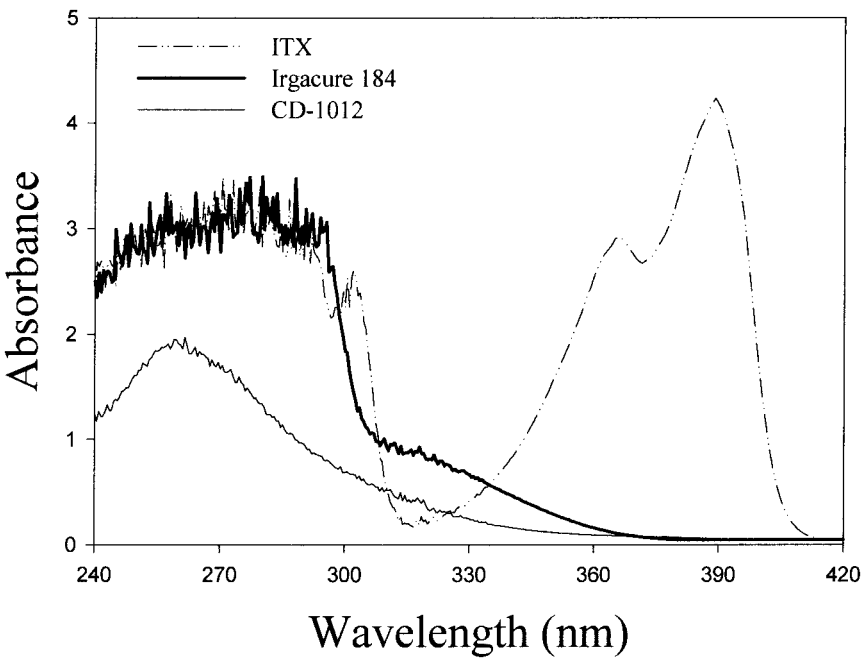

Figure 5 Absorption spectra of the photoinitiators (Irgacure 184, CD-1012) and photosensitizer (ITX).

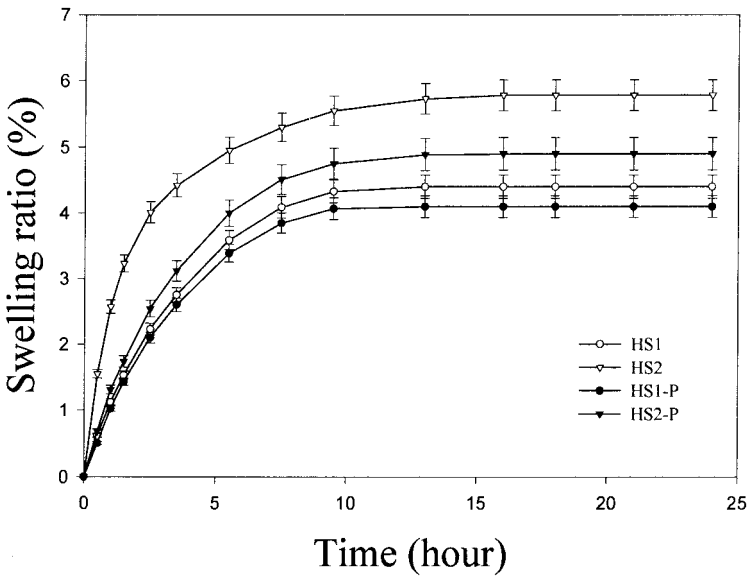

Figure 6 Swelling ratio of the hybrid systems with and without photosensitizer (HS1, HS1-P: acrylate/epoxide system; HS2, HS2-P: acrylate/vinyl ether system) as a function of time.

Figure 7 illustrates the photo-DSC exotherms for the photopolymerizations of the CS, RS, and HSs (HS1, HS2). Figure 8 shows the comparison of the photo-DSC exotherms for the photopolymerizations of the HSs with and without photosensitizer. The amount of heat released, the induction time, the peak maximum, the ultimate percentage conversion, and the maximum polymerization rate, $R_{p,max}$, derived from Figures 7 and 8, are collected in Table IV.

Comparison of the experimental results for the CS and the RS in Figure 7 and Table IV reveals that the exotherms and percentages converted (which are related to the crosslink density) of the CS are lower than those of the RS. Interestingly, these results are contrary to the pendulum hardness and Izod impact test results (which are also related to the crosslink density) shown in Table II. This discrepancy may be explained by the experimental results in Table II being obtained 24 h after the UV curing, and hence the unreacted

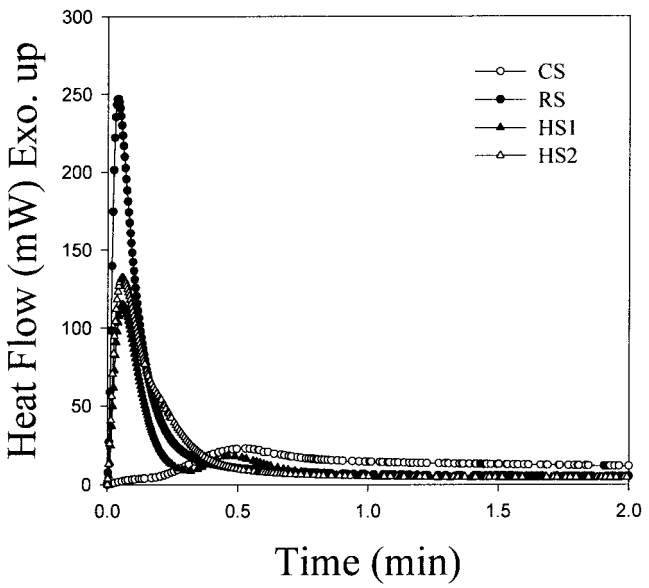

Figure 7 Photo-DSC exotherms for the photopolymerization of cationic (CS), free radical (RS), and hybrid (HS1, HS2) system formulations, under the following conditions: sample weight 4.0 mg, sample thickness ~ 500 μm, light intensity 35 mW/cm^2, and isothermal curing at 40°C.

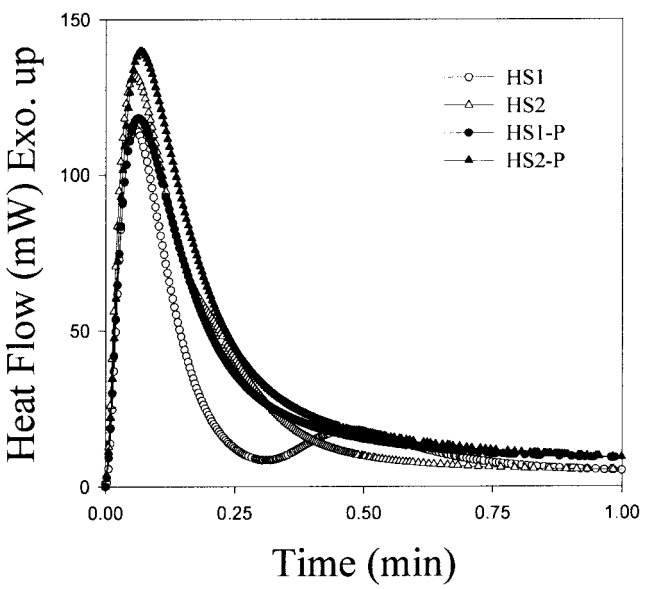

Figure 8 Photo-DSC exotherms for the photopolymerization of hybrid coating formulations with (HS1-P, HS2-P) and without (HS1, HS2) photosensitizer, under the conditions described in the legend to Figure 7.

TABLE IV
Exothermic Results Calculated with Photo-DSC Experiment for the Photopolymerization of Cationic, Free Radical, and Hybrid Formulations in Table I[a]

Formulation	ΔH (J/g)	Induction time (s)	Peak maximum (min)		Conversion (%)	$R_{p,max}$[b] (l/min)
			First	Second		
CS	255	8.41	0.52	—	39	0.64
RS	503	1.10	0.05	—	77	7.35
HS1	349	2.02	0.07	0.21	53	5.05
HS2	403	1.83	0.07	0.47	62	5.18
HS1-P	415	2.17	0.08	—	64	4.16
HS2-P	479	1.95	0.09	—	73	4.24

[a] Conditions are as described in the legend to Figure 7.
[b] $R_{p,max}$, Maximum polymerization rate ($R_p = d\alpha/dt$, where α is the converted fraction of resin).

epoxide (CADE) and VE (CHVE) groups would have continued to react slowly upon storage of the sample in the dark, thereby leading to the more highly crosslinked polymer networks: dark curing (or postpolymerization) is a distinct characteristic of cationic photopolymerizations.[14–16] Dark curing of the samples did not occur during the photo-DSC experiments. This interpretation is supported by the observation that this postreaction did not occur near the bottom of the samples.[5,14] In comparing reactivity, as expected, the RS exhibited a shorter induction time (which is related to the efficiency of the photoinitiator) and a lower peak maximum as well as higher $R_{p,max}$ than did the CS, which implies that the polymerization reactivity of the RS is much faster than that of the CS. The HSs were also shown to polymerize faster than the CS. Consequently, these HSs overcame the disadvantageous slow curing rate of the CS.

From Figure 8 and Table IV, it is interesting to note that the exotherms of the HS1 and HS2 HSs without photosensitizer exhibited two peaks, which reflect that they may produce IPNs and that their formulation components exhibited substantial differences in reactivity. The bimodal exotherms clearly demonstrate that the radical-induced polymerization of the acrylate takes place before the cationic-induced polymerization of the epoxide and VE. On the other hand, the exotherms of HS1-P and HS2-P (containing photosensitizer) showed only one peak. This behavior can be attributed to the epoxide and VE in the HSs polymerizing more rapidly due to the aforementioned photosensitization effect.

One further interesting phenomenon is that the photosensitized HSs exhibited higher induction time and peak maximum and a lower $R_{p,max}$ than did the nonphotosensitized HSs. It is attributable to chain mobility restrictions brought upon by the epoxide or VE network rapidly performed by the photosensitization, which slows down the polymerization rate of the acrylate during the early stage of irradiation. However, the presence of ITX photosensitizer was found to increase the overall amount of heat released as well as the ultimate percentage conversion of the photosensitized HSs, most probably because of the photosensitization effect. This tendency reflects the better performance of formulations HS1-P and HS2-P in the experimental results shown in Table II—the addition of ITX photosensitizer effectively enhances the physical properties of the HSs.

It should be noticed from Figure 8 and Table IV that the amount of heat released and the ultimate percentage conversion were lower for HS1 than for HS2. These results are contrary to the pendulum hardness and Izod impact test results presented in Table II. As in the CS and RS, this may be due to differences in the extent of dark curing between the HSs. An experiment was designed using DSC on the UV-cured sample immediately after the photo-DSC experiments to investigate the dark-curing processes of HS1 and HS2 (the experimental conditions are outlined in the DSC experiment in Section 2).

Figure 9 indicates that the chemical reaction was more exothermic for HS1 than for HS2 when the samples were

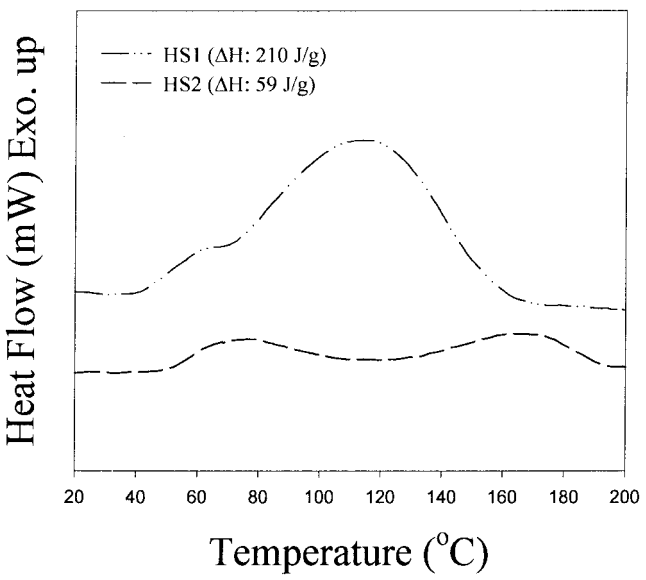

Figure 9 DSC exotherms for the hybrid formulations (HS1, HS2) immediately after the photo-DSC experiments.

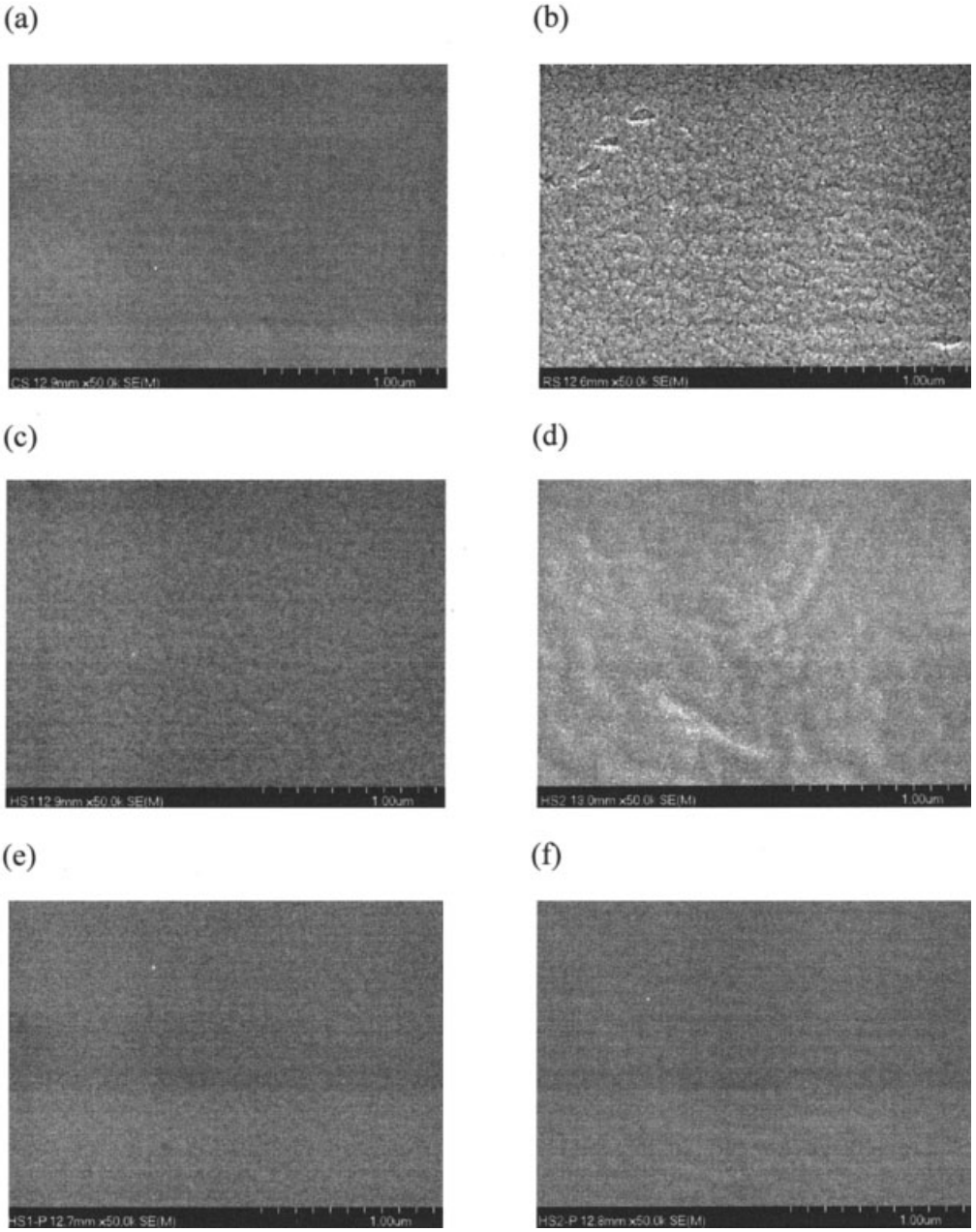

Figure 10 Scanning electron micrographs at the film–air interface of the UV-cured films: (a) CS, (b) RS, (c) HS1, (d) HS2, (e) HS1-P, and (f) HS2-P.

heated, which means that the amount of unreacted epoxides remaining in the HS1 sample was greater than the amount of unreacted VEs remaining in the HS2 sample. Therefore, after the completion of polymerization in the dark, HS1 exhibited better physical properties than did HS2, as indicated in Table II. Thus, the DSC analysis allowed us to monitor the dark-curing processes occurring in the HSs investigated in this study.

Surface morphology

We used SEM to investigate the effects of oxygen inhibition and photosensitization on the surface morphology of the UV-cured films at the film–air interface. SEM micrographs of the surfaces of the various UV-cured films are shown in Figure 10. The surface of the CS is relatively smooth, since it is not affected by oxygen inhibition [Fig. 10(a)]. In contrast, the very rough surface of the RS is ascribed to the presence of oxygen inhibition [Fig. 10(b)]. From Figures 10(c) and (d), it can be also seen that the A/E (HS1) and A/VE (HS2) HSs exhibited better surface morphology than did the RS, and also that the surface of the HS1 is smoother than that of the HS2. These observations confirm that the HSs overcome the oxygen inhibition that is common to RSs and that the extent of cure at the

surface of the UV-cured film for HS1 was greater than for HS2. This is consistent with the pencil hardness and MEK solvent resistance test results listed in Table II. The HSs containing photosensitizer [HS1-P and HS2-P, in Fig. 10(e) and (f), respectively] show surface morphology superior to those of HS1 and HS2 containing no photosensitizer, and their surfaces are as smooth as that of the CS. These results clearly indicate that the addition of ITX photosensitizer enhanced the surface curing of the HSs.

CONCLUSION

UV-initiated acrylate (TMPTA)/epoxide (CADE) and urethane acrylate (UA)/VE (CHVE) hybrid photopolymerizations with and without photosensitizer (ITX) have been studied by DMTA, calorimetric analysis (using photo-DSC and DSC), and SEM. The oxygen inhibition seemed to be lower in the HSs than in the RS, and the cure rate was faster in the HSs than in the CS. DMTA experiments showed that the UV curing of HSs may produce IPNs and that the crosslink density was higher in the A/E (HS1) HS than in the A/VE (HS2) HS. Photo-DSC analyses indicated that the acrylates polymerized faster than the epoxide and VE in the HSs and that the addition of ITX increased the polymerization rate of the epoxide and VE in the HSs. DSC experiments allowed us to effectively monitor the postpolymerization process occurring in the HSs. SEM analysis confirmed that the RS was significantly affected by oxygen inhibition, while the CS and HSs were not nearly inhibited by oxygen; moreover, the presence of photosensitization produced by the addition of ITX enhanced the surface curing of the HSs.

References

1. Dietliker, K. K. In Chemistry and Technology of UV and EB Formulation for Coatings Inks and Paints; Oldring, P. K. T., Ed.; SITA Technology: London, 1991; vol. 3.
2. Jurczak, E. A. Proceedings of the RadTech North America Conference: Chicago, 1996; pp. 351–360.
3. Oldring, P. K. T., Ed. Chemistry and Technology of UV and EB Formulation for Coatings Inks and Paints; SITA Technology: London, 1991; vols. 1–4.
4. Roffey, C. G., Ed. Photopolymerization of Surface Coatings; Wiley: New York, 1982.
5. Nelson, E. W.; Carter, T. P.; Scranton, A. B. Macromolecules 1994, 27, 1013.
6. Decker, C.; Viet, T. N. T.; Decker, D.; Weber-Koehl, E. Polymer 2001, 42, 5531.
7. Shaobing, W.; Matthew, T. S.; Mark, D. S.; William, J. S. Polymer 1999, 40, 5675.
8. Decker, C.; Decker, D.; J Macromol Sci, Pure Appl Chem, A 1997, 34, 606.
9. Dougherty, J. A.; Vara, F. J. Mod Paint Coat 1991, 81, 42.
10. Sitzmann, E. V.; Anderson, R. F.; Cruz, J. G.; Bratslavsky, S. A. Haynes, R. L. Proceedings of the RadTech North America Conference: Chicago, 1998, pp. 53–64.
11. Fouassier, J. P.; Rabek, J. F., Eds. Radiation Curing in Polymer Science and Technology; Elsevier Applied Science: London, 1993; vol. I.
12. Nakamura, Y.;Yamaguchi, M.; Kitayama, A.; Ito, K. J Appl Polym Sci 1990, 39, 1045.
13. Vabrik, R., Czajlik, I.; Tury, G.; Rusznak, I.; Ille, A.; Vig, A. J Appl Polym Sci 1998, 68, 111.
14. Cho, J. D.; Kim, E. O.; Kim, H. K.; Hong, J. W. Polym Test 2002, 21, 781.
15. Cho, J. D.; Kim, H. K.; Kim, Y. S.; Hong, J. W. Polym Test 2003, 22, 633.
16. Decker, C.; Moussa, K. J Polym Sci, Part A: Polym Chem 1990, 28, 3429.
17. Hill, L. W. J Coat Technol 1992, 64, 29.
18. Wu, S.; Jorgensen, J. D.; Soucek, M. D. Polymer 2000, 41, 81.
19. Sperling, L. H., Ed. Introduction to Physical Polymer Science; Wiley: New York, 1992, Chaps. 8 and 9.
20. Hacker, M. P. Proceedings of the RadTech Asia Conference: Tokyo, 1993; pp. 114–121.
21. Dektar, J. L.; Hacker, N. P. J Photochem Photobiol A Chem 1989, 46, 233.
22. Anderson, V. S.; Norrish, R. G. W. Proc R Soc Lond 1959, 51, 1.
23. Manivannan, G.; Fouassier, J. P. J Polym Sci, Part A: Polym Chem 1991, 29, 1113.
24. Nelson, E. W.; Carter, T. P.; Scranton, A. B. Proc Am Chem Soc Polym Mater Sci Eng 1993, 69, 363.
25. Clark, S. C.; Hoyle, C. E.; Jonsson, S.; Morel, F.; Decker, C. Polymer 1999, 40, 5063.
26. Pogue, R. T.; Ullett, J. S.; Chartoff, R. P. Thermochim Acta 1999, 339, 21–27.